Biomass Conversion and Biorefinery (2024) 14:133–146
https://doi.org/10.1007/s13399-021-02184-4

ORIGINAL ARTICLE

Leaching mechanisms of ash-forming elements during water washing of corn straw

Yuefeng Wang[1] · Shugang Guo[2] · Fang Cao[1] · Chong He[1] · Yuexing Wei[1] · Yuhong Qin[1] · Yanyun He[1] · Xing Du[2] · Stanislav V. Vassilev[3] · Christina G. Vassileva[3]

Received: 23 September 2021 / Revised: 1 December 2021 / Accepted: 2 December 2021 / Published online: 13 January 2022

Abstract

One of the challenges for large-scale biomass gasification is inevitable ash-related problems such as ash deposition, corrosion, fouling, acid gas emission, and others, mainly caused by the volatile ash-forming elements in biomass. Water washing is an efficient, low-cost, and manageable way to alleviate these ash-related problems by reducing the concentrations of ash-forming elements in biomass. The leaching characteristics of ash-forming elements such as K, Na, Ca, Mg, Al, Fe, S, Cl, and P of corn straw (CS) were studied by inductively coupled plasma mass spectrometry (ICP-MS), ion chromatography (IC), and ultraviolet–visible spectroscopy (UV–Vis) during water washing at different time and temperatures. It was found that the water washing process removes almost all of K, Cl, and P with a removal efficiency higher than 90% within the first 10 min; large proportions of S, Na, and Mg with a removal efficiency of more than 70% within 120 min; and small amounts of Ca, Al, and Fe with a removal efficiency less than 63% within 120 min even at 50 ℃. The kinetic analysis indicated that the leaching of ash-forming elements was a two-step process consisting of an initial fast step and a second slow step. The leaching of ash-forming elements might be controlled by the first-order kinetic model, namely, homogeneous model and shrinking core model. Still, the second-order reaction model presents high regression coefficients, which is better suitable to fit the leaching kinetics of ash-forming elements from CS than the first-order kinetic leaching model. The reaction rate for the second-order reaction is faster than the first-order reaction during the water leaching of CS. The water washing could reduce the slagging tendency in the gasifier and diminish the emission of acid gases during corn straw gasification.

Keywords Corn straw · Water washing · Ash-forming elements · Leaching kinetic

1 Introduction

Biomass gasification is considered one of the most promising technologies for power generation and production of chemicals in the near future. Among the biomass-to-electricity conversion technologies, biomass-based integrated gasification combined cycle (BIGCC) has been proposed and demonstrated since the 1990s due to the number of low pollutants released, low electricity generation cost, as well as high power efficiency [1–4]. However, the ash deposition, air pollution, and high-temperature corrosion caused by ash inhabit the stable operation of biomass power plants [5, 6]. High contents of ash-forming elements such as Cl, S, K, Na, N, and P from biomass should account for those ash-related operational and environmental problems. Volatile alkali metals commonly form molten salt mixtures of hydroxides, chlorides, and sulfates, which are responsible for slagging and fouling during the gasification process [7–10]. Chlorine in biomass is considered a promoter of alkali metals evaporation, and its abundance will lead to the condensation and deposition of alkali chlorides on heating surfaces in the boiler. The severe deposition not only reduces the heat transfer but also causes boiler shutdown irregularly [11–13]. Furthermore, N, S, and Cl in biomass are normally

✉ Yuhong Qin
qinyuhong@tyut.edu.cn

1 College of Environmental Science and Engineering, Taiyuan University of Technology, 79 Yingze West Street, Taiyuan 030024, People's Republic of China

2 Shanxi Provincial Center for Disease Control and Prevention, 8 Xiaonanguan Street, Taiyuan 030012, People's Republic of China

3 Institute of Mineralogy and Crystallography, Bulgarian Academy of Sciences, Acad. G. Bonchev Street, Block 107, Sofia 1113, Bulgaria

discharged by the formation of NO_X, SO_X, HCl, dioxins, and particulates during the thermal conversion process, thus leading to air pollution. In addition, the above-mentioned inorganic species can poison catalysts in the downstream process, resulting in catalyst deactivation [14–16]. Therefore, it is beneficial to remove some inorganic elements from biomass before gasification.

Water washing is an efficient, low-cost, and manageable way to remove ash-forming elements from biomass, which is favorable for solving ash melting and fouling problems [6, 7, 17, 18]. It is commonly accepted that some ash-forming elements in biomass can be removed by water washing, and the leaching ability of water varies within the elements [19, 20]. For instance, K, Na, and Cl show high solubility, and Mg is more soluble than Ca, while both alkaline-earth elements are less leachable than the alkaline metals [21]. The water solubility of P and S appear to be fuel dependent due to their highly variable contents in biomass [16, 22]. For example, P in agricultural residues shows high solubility (> 50%) [23]. The solubility of S in wheat straw, rice straw, and almond hulls are higher than that in woody biomass fuels [6, 22, 24]. Werkelin et al. [25] proved that the water-soluble Cl and S are mainly presented as Cl^- and SO_4^{2-} in leachate, respectively. Deng et al. [26] concluded that C and P were leached with HCO_3^-, $H_2PO_4^-$ and HPO_4^{2-} in the leachate during water washing of a set of biomasses. Summarized reference data [9] show that the water-soluble elements leached from numerous biomasses are mainly Cl, S, N, P, K, Na, Mg, and Mn, and to a lesser extent, Ca, Al, Fe, and Si. It is evident that most studies were focused on specific leachable elements. However, it is also important to have a comprehensive study on the leaching characteristics of the major and minor ash-forming elements of biomass.

The ash-forming elements exist as organic matter, salts, and minerals in the biomass. In addition to inorganic species, some organic compounds such as organic acids, carbohydrates, ethanol, and others in biomass can also be washed out by water [17, 27]. However, certain organically bound alkaline-earth species are difficult to be fully leached by water [28]. Some researchers connected the change of pH and electrical conductivity of the leachate with the anion and cation leaching behavior [25, 29, 30]. For instance, Stanković et al. [29] found that the pH value of the leachate increased from 5 to 6 due to the replacement of H^+ by Ca^{2+} during the water washing of sawdust and wheat straw. In contrast, the leaching of organic acids such as acetate, formate, and oxalate ones causes a pH decrease from 6.3 to 5.5 and even to 4.2 during batch water leaching of the wood and leaf [5]. The acidic leachate could increase the leaching efficiency of some ash-forming elements. Madanayake et al. [30] found that the leaching process was completed when the electrical conductivity was approximately constant. It was concluded that the change of pH value and electrical conductivity of leachate, which is caused by the interaction between the anions and cations, is also associated with the leaching characteristics of biomass. However, studies about the effect of interactions between anions and cations in the leachate on the leaching of ash-forming elements were scarce.

The leaching rate and the interactions between anions and cations during biomass washing are vital to understanding the leaching process. Several attempts have been made to study the kinetic behavior of water leaching systems to provide a scientific basis for the optimization of washing conditions. Ho et al. [31] proposed a second-order kinetics model for the batch leaching of water-soluble compounds in *Tilia* sapwood and revealed the kinetic parameters of different water-soluble compounds. Liaw et al. [5] studied the leaching kinetics of K, Na, Ca, and Mg in semi-continuous water leaching and found that the leaching kinetics of these elements belong to the first-order kinetics, which includes the one-step leaching process. Schmidt et al. [32] established first- and second-order kinetic models to simulate the ionic exchange between water and wood based on the variation of electrical conductivity with time. Previous studies focused on the leaching kinetics of either water-soluble compounds or the ease of leaching elements instead of water-insoluble elements during different washing processes.

However, a comprehensive study regarding the leaching characteristics of the most ash-forming elements is still lacking. China is one of the biggest agricultural countries, and it is abundant in agricultural biomass residues. For example, a total of 889 million tons of agricultural biomass residues are produced per annum in China, and about 80% of them are corn and wheat straws [33]. The corn straw is the primary agricultural biomass residue in the Shanxi province which is located in the north of China [34]. The purpose of this study is to evaluate:(1) the leaching characteristics of ash-forming elements in corn straw, namely K, Na, Ca, Mg, Al, Fe, S, Cl, and P; and (2) the leaching kinetics and mechanisms of these elements; and (3) the possible ash-related problems during the gasification of this biomass.

2 Experimental

2.1 Sample

Corn straw (CS) collected from Taiyuan suburb (Shanxi province, China) was ground and sieved to a particle size of 150–180 μm. The proximate and ultimate analyses of the sample are given in Table 1. The determination of volatile matter and fixed carbon was conducted in accordance with ASTM D3175. Ash yield was determined at 575 ± 25 °C for 3 h according to ASTM E1755. Moisture content was measured

Table 1 Proximate and ultimate analyses of corn straw

Sample	Proximate analysis/wt.%				Ultimate analysis (db)/wt.%				
	M_{ad}	A_{db}	V_{db}	FC_{db}	C	H	O*	N	S
Corn straw	7.74	5.35	71.36	23.29	44.2	6.04	48.66	0.98	0.12

M moisture; *A* ash; *V* volatile; *FC* fixed carbon; *ad* air-dried basis; *db* dry basis; *By difference

Table 2 Contents of ash-forming elements in corn straw (wt.%, ad)

Element	Si*	Al	K	Na	Ca	Mg	Fe	S	P	Cl
Content	2.78	0.03	1.47	0 .03	0.28	0.22	0.02	0.14	0.07	0.07

*Si was analyzed with molybdenum blue method by UV–Vis spectra

corresponding to ASTM E1756-08. The ultimate analysis was analyzed by Vario EL cube elemental analyzer, Germany.

2.2 Water-leaching experiment

Nine ash-forming elements, namely K, Na, Ca, Mg, Al, Fe, S, Cl, and P in CS were leached by water with washing times of 3, 5, 6, 10, 20, 30, 40, 60, 80, 100, and 120 min, separately. The washing temperature used was 20 ℃ and 50 ℃ based on the cooling temperature of water in the power plant [6]. The leaching test was performed using 2.0 g of corn straw and 200 mL ultrapure water in a beaker under continuous stirring for a specific time at 20 ℃ or 50 ℃. After the leaching test, the mixture was filtrated and separated into the leached corn straw (LCS) and its leachate. LCS was dried in an oven at 105 ℃ for 2 h, then weighted, and dried again until a constant weight was maintained. Dried LCS was stored in a desiccator. All the experiments were performed at least three times to minimize experimental errors. The average test values were used herein.

2.3 Quantitative determination of ash-forming elements in corn straw

The ash-forming elements in LCS and CS such as K, Na, Ca, Mg, Al, and Fe were analyzed by inductively coupled plasma mass spectrometry (ICP-MS), model iCAQ, Thermo scientific, USA. The SO_4^{2-} and Cl^- anions were determined using ion chromatograph (IC), model DIONEX ICS-2100, Thermo scientific, USA. The IC apparatus was equipped with a suppressed conductivity detection system (AERS 500). The separation was achieved by IonPacTM AS19-4 mm analytical column equipped with an IonPac AG19-4 mm guard column using 17 mM KOH as eluent. The flow rate of eluent was 1.0 mL/min, and the detection volume was 25 µL. Column temperatures were maintained at 30 ℃ and the suppressor current at 30 mA. Phosphorous was determined by ultraviolet visible spectrophotometer (UV–Vis), model UV 2450, Shimadzu, Japan. Each element was calibrated using K, Na, Ca, Mg, Al, Fe, P, Cl^- and SO_4^{2-} standard stock solutions. Quantification of all elements is based on the standard curve method. The standard curve can cover the entire concentrations range of unknown samples.

2.4 Other digestion procedures

A digestion experiment was conducted with LCS and raw CS before using ICP-MS, IC and UV–Vis analyses. Approximately 0.2 g of LCS and CS samples were digested with 6 mL of concentrated nitric acid (HNO_3, 68% w/w, GR), 0.5 mL of hydrogen peroxide (H_2O_2, 30% w/w, AR) at 160 ℃ for 4 h. The digestion tank was placed in a fume hood after digestion to reduce the volatile concentration. Finally, the solution was diluted to 50 mL with HNO_3 (5%, v/v) and stored in a refrigerator at -4 ℃ before analysis. The digested solution was filtered through a 0.45 µm syringe filter to remove microparticles before IC test. The ash-forming elements of CS analyzed by the above methods are listed in Table 2.

2.5 Data analysis method

In order to analyze and compare the leaching efficiency of different elements, the removal efficiency X_i (%) of a certain element defined as Eq. (1), where i represents the elements (K, Na, Ca, Mg, Al, Fe, P, Cl, and S).

$$X_i = \left(1 - \frac{M_{LCS,\,d} \times Y_{LCS,\,i}}{M_{CS,\,d} \times Y_{CS,\,i}}\right) \times 100\% \quad (1)$$

where, $M_{CS,\,d}$ and $M_{LCS,\,d}$ are the mass of CS and LCS sample, dry basis, g; $Y_{CS,\,i}$ and $Y_{LCS,\,i}$ are the mass concentration of the element i in the CS and LCS sample, μg/g. Different elements i are detected by different instruments, $Y_{CS,\,i}$ and $Y_{LCS,\,i}$ has different calculation methods as follows:

For the data from ICP-MS analysis, the element i contains K, Na, Ca, Mg, Al and Fe, $Y_{CS,\,i}$ and $Y_{LCS,\,i}$ can be calculated according to Eq. (2).

$$Y_{CS,\,i}\left(Y_{LCS,\,i}\right) = \frac{\left(C_i - C_{0,\,i}\right) \times V_1}{M_{digestion,\,d}} \tag{2}$$

where, C_i is the concentration of the element i getting from ICP-MS instrument, μg/mL; $C_{0,\,i}$ is the concentration of elements i for blank solution, μg/mL; V_1 is the volume of sample solution before analyzing with ICP-MS and IC, 50 mL; $M_{digestion,\,d}$ is the mass of digested CS and LCS sample, dry basis, g.

The elements S and Cl were analyzed by IC in the forms of Cl^- and SO_4^{2-}. The values of $Y_{CS,\,Cl}$ and $Y_{LCS,\,Cl}$ can be obtained according to the Eq. (2). The calculation of $Y_{CS,\,S}$ and $Y_{LCS,\,S}$ needs to be converted from $SO4^{2-}$ as shown in Eq. (3) and Eq. (4).

$$Y_{CS,\,SO_4^{2-}}\left(Y_{LCS,\,SO_4^{2-}}\right) = \frac{\left(C_{SO_4^{2-}} - C_{0,\,SO_4^{2-}}\right) \times V_1}{M_{digestion,\,d}} \tag{3}$$

$$Y_{CS,\,S}\left(Y_{LCS,\,S}\right) = Y_{CS,\,SO_4^{2-}}\left(Y_{LCS,\,SO_4^{2-}}\right) \times \frac{W_S}{W_{SO_4^{2-}}} \tag{4}$$

where $Y_{CS,\,SO_4^{2-}}$ and $Y_{LCS,\,SO_4^{2-}}$ are the mass concentration of the SO_4^{2-} in the CS and LCS sample, μg/g; $C_{SO_4^{2-}}$ is the concentration of the SO_4^{2-} for sample solution, μg/mL; $C_{0,\,SO_4^{2-}}$ is the concentration of the blank solution, μg/mL; W_S is the molar mass of S, 32 g/mol; $W_{SO_4^{2-}}$ is the molar mass of SO_4^{2-}, 96 g/mol.

The element P was analyzed with a UV–Vis spectrometer. The values of $Y_{CS,\,P}$ and $Y_{LCS,\,P}$ were calculated based on Chinese national standard GB 5009.87–2016 as shown in Eq. (5).

$$Y_{CS,\,P}\left(Y_{LCS,\,P}\right) = \frac{\left(M_P - M_{0,\,P}\right) \times V_2}{M_{digestion,\,d} \times V_3} \tag{5}$$

M_P is the mass of sample solution of element P, μg, dry basis; $M_{0,\,P}$ is the mass of blank solution, μg, dry basis; V_2 is the sample volume to be measured for the molybdenum blue spectrophotometry, 2 mL; V_3 is the sample volume after digestion for measuring P, 10 mL.

2.6 Kinetic model

The fluid–solid reactions were involved during the water washing of corn straw. For the non-catalytic reaction of particles surrounded by a fluid, the most commonly used two models, namely the first-order kinetic model, including a homogeneous model and a shrinking nucleus model, as well as a second-order kinetic model, which were adopted for studying the leaching of ash-forming elements. The leaching process was simply assumed to proceed as:

$$\text{Corn straw}_s + \text{Water}_1 \leftrightarrow (\text{Water} - \text{soluble compounds})aq + (\text{Leasched corn straw})_s$$

The homogeneous model assumes that the leaching of ash-forming elements from CS into the leachate is uniform [35]. The model presumed that the particle size of CS does not change during the water washing process. If the leaching process follows the homogeneous model, it can be described by the following Eq. (6).

$$-\text{Ln}(1 - X_i) = K_a \times t \tag{6}$$

where, K_a is the reaction constants, min^{-1}; t is the washing time, min; X_i is the removal efficiency calculated by Eq. (1). The shrinking core model for leaching of ash-forming elements is based on the following assumptions: the CS particles have a spherical geometry; the leaching reaction of the ash-forming elements initially occurs at the external surface of the CS and gradually moves inside [36]. The core of non-reacted CS shrinks during the water washing. The shrinking core model can be divided into the following several steps: (1) leaching-agent (H_2O) molecule diffuses to the surface of CS; (2) the portions of ash-forming elements are dissolved and diffused through the diffusion layer; (3) the ash-forming elements diffuse into the leachate. In this study, the diffusion layer is a condensed liquid owing to the high solubility of the leached ash-forming elements. The extra stirring eliminates the influence of external diffusion resistance. When the leaching of ash-forming elements is controlled by the interaction of leachate and CS particles, the model is represented by Eq. (7) [36], where K_c is the rate constant of the reaction control process.

$$1 - \left(1 - X_i\right)^{1/3} = K_c \times t \tag{7}$$

When the diffusing process of ash-forming elements becomes a rate-controlling step, the process is described as following Eq. (8) [36]. K_p is the rate constant of the diffusion-control process.

$$1 - \frac{2X_i}{3} - \left(1 - X_i\right)^{2/3} = K_p \times t \tag{8}$$

The removal efficiency of the ash-forming elements from CS water washing showed a general trend which is initially fast and followed by a slow leaching step. Therefore, a second-order leaching model would reasonably describe the leaching kinetics of the ash-forming elements in CS. The second-order leaching model is shown in Eq. (9). Integrated rate law Eq. (10) can be obtained by integrating Eq. (9) with the boundary condition t = 0 to t. Rearrangement of Eq. (10) gives its linear form Eq. (11). By fitting the data into t versus t/C_t, leaching parameter C_s can be obtained from the slope, and K can be calculated from the intercept [31, 37, 38].

$$\frac{dC_t}{dt} = K(C_s - C_t)^2 \tag{9}$$

$$C_t = \frac{C_s^2 Kt}{1 + C_s Kt} \tag{10}$$

$$\frac{t}{C_t} = \frac{t}{C_s} + \frac{1}{KC_s^2} \tag{11}$$

where K is the second order leaching rate constant ($L \cdot mg^{-1} \cdot min^{-1}$); C_s is the equilibrium concentration ($mg \cdot L^{-1}$) and C_t is the concentration ($mg \cdot L^{-1}$) of ash-forming elements in water at time t.

3 Results and discussion

3.1 Leaching character of ash-forming elements

The removal efficiency of nine ash-forming elements calculated from Eq. (1) at different washing times and washing temperatures are shown in Fig. 1. Results reveal that these elements can be divided into three categories based on their removal efficiencies at 20 ºC and 50 ºC. The type I includes K, Cl, and P. These elements are highly soluble in water and their removal efficiency is greater than 90% within the first 10 min and keeps steady within 120 min. The type II comprises of Na, Mg, and S. These elements have a removal efficiency greater than 70% within 120 min. The removal efficiency of the type III elements such as Ca, Fe, and Al is less than 63% within 120 min, even at 50 ºC.

3.1.1 Leaching character of K, Cl, and P

The removal efficiency X_i of ash-forming elements during the water-washing process mainly depends on the modes of element occurrence in CS, liquid–solid ratio, water-washing temperature and time. The inorganic matter in biomass occurs in the following forms: ionic-bound salts, organic-bound elements, and/or included and excluded mineral

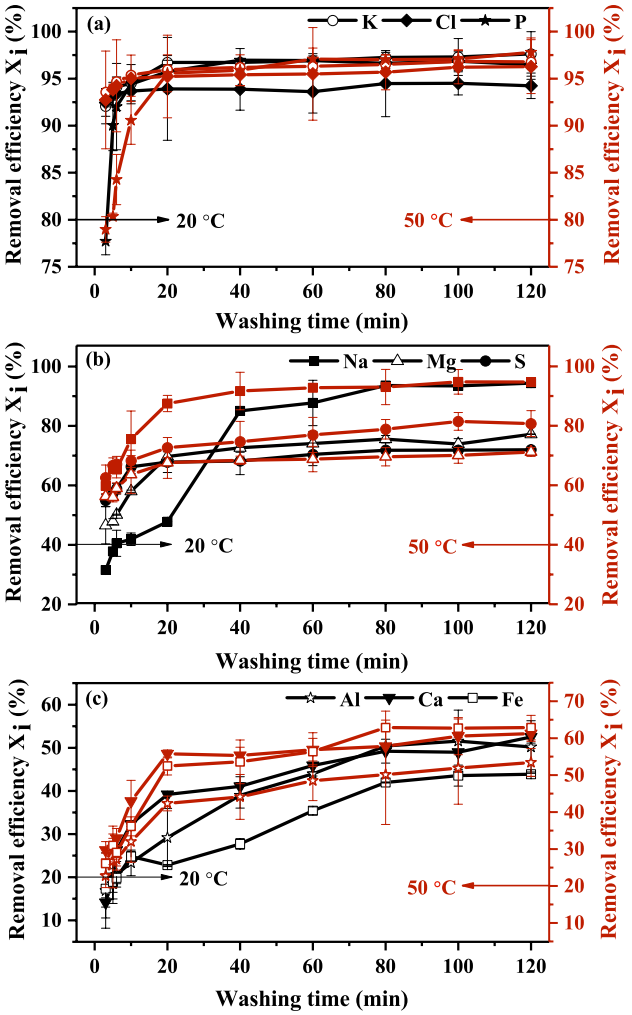

Fig. 1 Removal efficiency of ash-forming elements at different temperatures and time (a) type I at 20 ºC and 50 ºC, (b) type II at 20 ºC and 50 ºC, (c) type III at 20 ºC and 50 ºC

matter [25]. As shown in Fig. 1a, both the removal efficiency of K and Cl are higher than 92% within 3 min at 20 ºC and 50 ºC. It indicates that the water-washing temperature has no responsibility for the leaching of K and Cl. Moreover, it shows the strong association between K and Cl as most of their proportions exist in an ionic-bounded mode in CS. This result is in agreement with other researchers' conclusions [6].

The X_P increases to 90% at 5 min and 20 ºC, and then rises slowly up to 97% before it keeps constant at 40 min, as shown in Fig. 1a. In contrast, the time of X_p reaching 90% at 50 ºC is 10 min, which is longer than that at 20 ºC. The leaching of P reaches equilibrium (96%) after 20 min water-washing process at 50 ºC. Most of P in CS exists in the form of water-soluble inorganic phosphates of K, Na, and ammonium, which are easily leached [25]. These phosphates are probably trapped in the organic structure and are

less mobile than K and Cl in CS. Further, the removal efficiency of P decreases as the temperature increases from 20 to 50 ºC. The specific X_P values at 20 ºC were 78%, 90%, 92%, and 94%, while at 50 ºC they were 79%, 80%, 84%, and 91% for 3 min, 5 min, 6 min, and 10 min, respectively. This phenomenon might be caused by initially competitive leaching among CO_3^{2-}, HCO_3^-, SO_4^{2-} with PO_4^{3-}, HPO_4^{2-}, $H_2PO_4^-$ at higher temperatures in order to keep the charge balance in the leachate. It seems that the inhibition effect was eliminated with the time extension.

3.1.2 Leaching character of Na, Mg, and S

As shown in Fig. 1b, the X_{Na} dramatically increases from 32% at 3 min to 94% at 80 min at 20 ºC, while it is 60% at 3 min and 92% at 40 min at 50 ºC, respectively. It is evident that both washing time and temperature have positive effect on the removal efficiency of Na. The leaching of Na in the early stage of water washing is probably related to inorganic Na compounds such as NaCl, Na_2CO_3, and NaOH, which are highly soluble in water. Some organically bound Na combined with malate, carboxyl and phenoloxy groups can also be leached over time [25]. Compared with the leaching characteristics of K, Na shows a different leaching behavior due to the difference in ion potential. The ion potential of Na is higher than K as the radius of Na ion is smaller than K ion. It results in the strengthened combination among Na^+ with ions such as Cl^-, CO_3^{2-}, CH_3COO^-, and other organic anions, which leads to the lower leaching rate of Na than K at the beginning of leaching time.

The leaching of Mg shows a similar removal trend to Na as the removal efficiency X_{Mg} increases sharply at the beginning 20 min and then increases slowly with time extension at both 20 ºC and 50 ºC. This observation indicates that most of Mg exists in the form of water-soluble salts, including $MgCl_2$, $MgSO_4$, and $Mg(NO_3)_2$ [39]. These Mg-containing compounds are easily leached during the initial water washing process. When the leaching time is prolonged, the acid groups such as CH_3COO^-, $C_2O_4^{2-}$, CO_3^{2-}, HCO_3^-, SO_4^{2-} and NO_3^- are formed and the weak acid environment in the leachate promotes the cation leaching of most metals. Interestingly, X_{Mg} at 20 ºC is lower than that at 50 ºC within 20 min. Conversely, X_{Mg} at 20 ºC is higher than at 50 ºC after 20 min. X_{Mg} reaches 77% at 20 ºC, while only 71% is obtained for X_{Mg} at 50 ºC for 120 min. It means that the increased temperature can improve the Mg removal efficiency in a certain time. It might be caused by the complicated interactions between cations and anions in the leachate which are intensified at higher temperatures with increasing time.

It can be seen in Fig. 1b that the leaching trend of S is similar to those of Na and Mg. The X_S increases with the leaching time due to the continuous leaching out of different sulfates for 120 min. Compared with the X_{Na} and X_{Mg} at 3 min, the initial X_S obtained at 20 ºC and 50 ºC are higher and show values of 55% and 63% respectively. The X_S increases by 17% when the washing time increases from 3 to 120 min, where X_S reaches 72% at 20 ºC and 81% at 50 ºC. It indicates that the temperature has a positive effect on the leaching of S; however, the leaching extent of this element is limited at the same leaching temperature. The increased extent of X_S is the smallest among type II elements with time on stream. The possible reason for that is the occurrence of some insoluble metal sulfides such as FeS_2, as well as S-containing protein that are difficult to remove during the water washing process.

3.1.3 Leaching character of Ca, Fe, and Al

The type III elements are the most difficult to dissolve compared with types I and II as shown in Fig. 1c. For example, X_{Ca} is less than 15% for 3 min and only 53% for 120 min at 20 ºC. X_{Ca} reaches 30% for 3 min and 61% for 120 min at 50 ºC. It indicates that the increment of temperature and time improves X_{Ca}. Compared with the other two types of elements, the low X_{Ca} is most likely related to the low solubility of Ca-containing compounds. The occurrence of Ca in corn straw may be as $CaCl_2$, $Ca(NO_3)_2$, $Ca(OH)_2$, $CaCO_3$, $CaSO_4$, and CaC_2O_4, as well as amorphous material with both organic and inorganic character [9]. It is well known that the solubility of $CaCl_2$ and $Ca(NO_3)_2$ increases with temperature, while the solubility of $Ca(OH)_2$ decreases with temperature. The solubility of both $CaCO_3$ and CaC_2O_4 increases with the washing time due to the increased concentration of H^+ in the leachate. Additionally, Ca-containing sulfate (gypsum), calcium silicate hydrate, and some organically bonded Ca have lower solubility in water [8].

As shown in Fig. 1c, X_{Fe} increases with increasing the washing time and temperature, namely: from 17% for 3 min to 42% for 80 min at 20 ºC; from 26% for 3 min to over 52% at 20 min; and 63% for 80 min at 50 ºC. Hence, the high temperature is favorable for the leaching extent of Fe. In contrast, the leaching behavior of Al is different from Ca and Fe. X_{Al} increases by more than 30% when the washing time increases from 3 to 120 min at 20 ºC and 50 ºC. The increase of X_{Al} is less than 13% when the washing temperature increases under the same washing time. It indicates that the leaching of Al is more sensitive to washing time. Elements Al and Fe in CS may occur in the forms of oxides, oxyhydroxides, silicates, sulfates, sulfides, and some chelates [39]. Except for the sulfates, the rest of these S-containing species are normally less soluble to insoluble in water.

The leaching characteristics of K, Na, Ca, Mg, Al, Fe, S, Cl, and P can provide theoretical guidance for the design of a water washing reactor and the optimization of water washing

conditions for the above ash-forming elements. For instance, K and Cl can be removed in a short period of time by the water spray method. Phosphorous can be leached more than 90% only for 10 min by soaking. Additionally, Na, Ca, Fe, and S leaching could be improved by increasing the washing time and temperature. Finally, the removal efficiency of Mg and Al can be significantly improved by using continuous leaching operations.

3.2 Cation–anion balances of leachate

In order to clarify the influence of other unanalyzed anions during the washing process, the balance of charge on anions and cations in the leachate under different washing conditions was investigated. It can be assumed that all leached elements are in the form of the highest valence charged ion groups except P. The leached Fe-and S-containing compounds exist in the forms of Fe^{3+} and SO_4^{2-} in the leachate. The P-containing groups are assumed to exist as HPO_4^{2-} because PO_4^{3-} is prone to hydrolysis into HPO_4^{2-} in water. Based on the above assumptions, the charge ratio of cation to anion can be represented as the ratio (Na + K + 2 Mg + 2Ca + 3Al + 3Fe)/(Cl + 2S + 2P) in the leachate. This charge ratio under different water washing times and temperatures is shown in Fig. 2. Its value exceeds 1 due to the presence of unanalyzed organic and inorganic anions in the leachate. The initial charge ratio is higher than 4.7 in the leachate, which is most likely caused by the leaching of HCO_3^- and CO_3^{2-}. Deng et al. [26] reported that C was leached mainly in the form of HCO_3^- at the beginning of washing. The charge ratio of cation to anion decreases within 6 min at 20 ℃ and 50 ℃ due to the rapid leaching of Cl^-, P^- and S-containing anions. Its value is above 4.6 and then keeps constant at 50 ℃. This may be caused by the increase of unanalyzed organic anions in the leachate associated with organic acids. The charge ratio of cation to anion in the leachate is less affected by the washing temperature, indicating that the temperature has limited influence on the leaching of the unanalyzed anions.

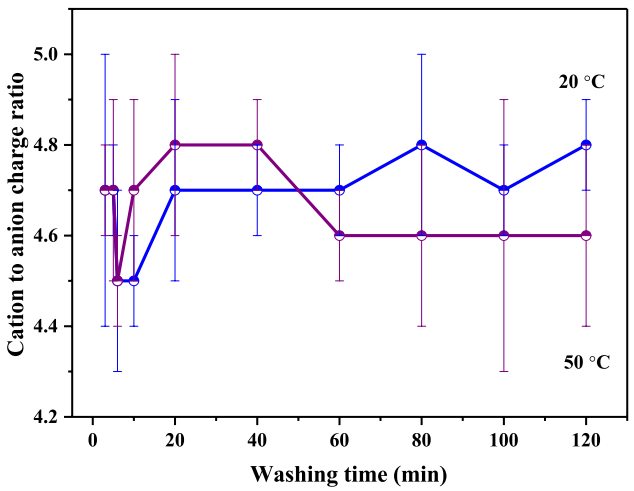

Fig. 2 The cation to anion charge ratio in the leachates with different washing time at 20 ℃ and 50 ℃

3.3 Leaching kinetics of ash-forming elements

To analyze the different leaching behavior of ash-forming elements, the removal efficiency trend with washing time was modeled with the first-order leaching model, including the homogeneous model (Eq. (6)) and the shrinking core model (Eq. (7) and Eq. (8)), as well as the second-order leaching model (Eq. (9–11)). The model process is shown in Fig. 3 at 20 ℃ and Fig. 4 at 50 ℃, separately. The comparison of the R^2 of the fitting equations from the first-order (R_1^2) and second-order kinetic (R_2^2) was shown in Table 3.

It can be seen (Fig. 3a) that the first-order leaching process of ash-forming elements includes two steps. The first step is a rapid leaching stage followed by the second step which is a slow leaching stage. The removal efficiency of type I elements such as K and Cl shows a good linear relationship with $1\text{-}2X_i/3\text{-}(1\text{-}X_i)^{2/3}$ from 3 to 120 min (Fig. 3a) with the regression coefficient R_1^2 of K and Cl higher than 0.92 (Table 3), while the R_1^2 of element P is lower with deviation from linearity. This observation indicates that the leaching of K and Cl is controlled by a diffusion process and can be described by the shrinking core model, but the behavior of P is less influenced by the above model. It is obvious that the leaching rate during the first step is greater than that of the second step. The first step corresponds to a rapid dissolution of water-soluble salts, while the second step involves the slow leaching of acid-soluble compounds. It can be seen (Fig. 3d and Table 3) that the R_2^2 of the fitted data of type I elements such as K, Cl, and P using a second-order leaching model is always 1.00. Therefore, the second-order kinetic model is better suitable to describe the leaching kinetics of type I elements from CS than the shrinking core model.

The type II elements such as Na, Mg, and S show dynamic leaching kinetics (Fig. 3b). For example, the leaching of Na and Mg are controlled by chemical reactions of shrinking core model with the regression coefficient R_1^2 of Na and Mg higher than 0.93 and 0.75 (Table 3), respectively. This observation shows that the fitting effect of Na is better than that of Mg. The reactions involved in the leaching process of Na and Mg include ion-exchange reactions between H^+ in the leachate and some ions in CS, hydrolysis of some salts, and other reactions. This leaching process consists of two distinct steps. The first leaching step of Mg proceeds for 20 min, while it is 40 min for the leaching of Na. The leaching time of Na in the first step is longer because the leaching

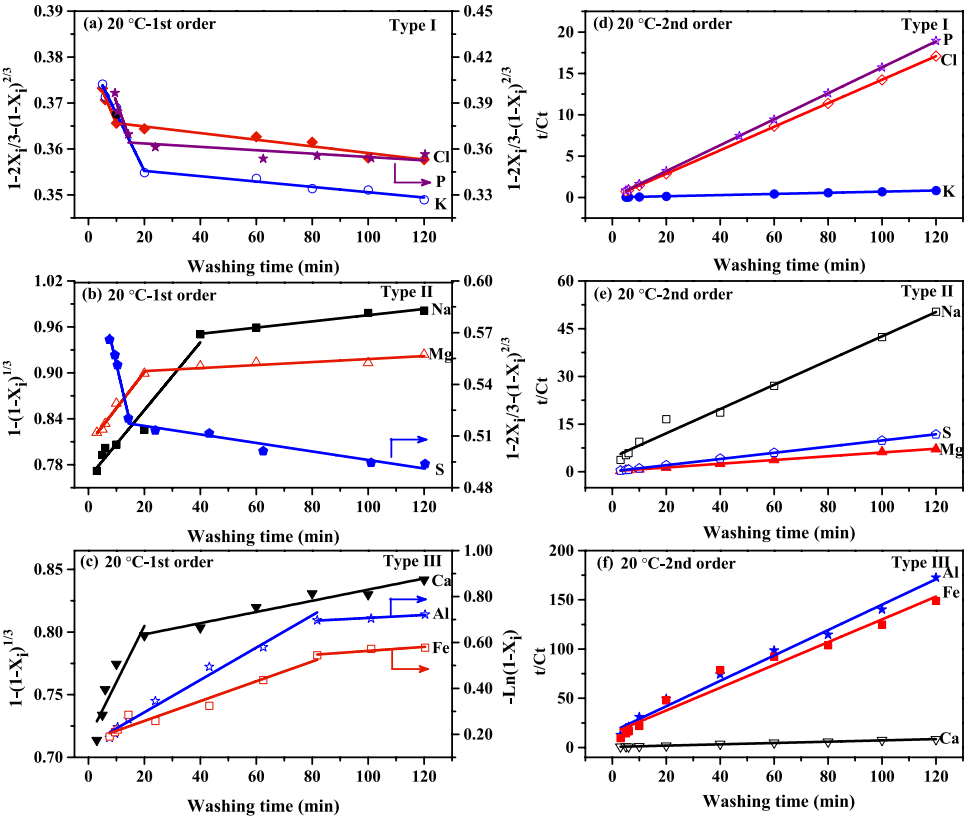

Fig. 3 The first-order (a, b, c) and second-order (d, e, f) leaching kinetics of ash-forming elements at 20 ℃

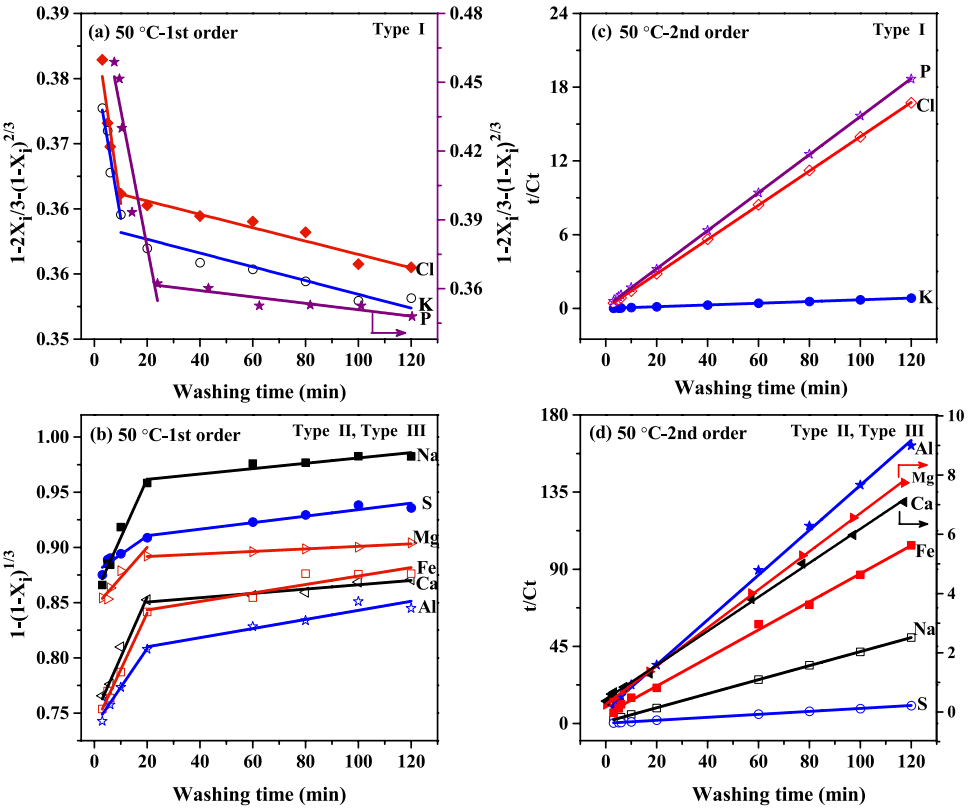

Fig. 4 The first-order (a, b) and second-order (c, d) leaching kinetics of ash-forming elements at 50 ℃

Table 3 Comparison of the R^2 of the fitting equations from the first-order and second-order kinetic

Element type		20 °C		50 °C	
		R_1^2	R_2^2	R_1^2	R_2^2
Type I	K	0.9760	1.0000	0.9141	1.0000
		0.9224		0.8583	
	Cl	0.9588	1.0000	0.8822	1.0000
		0.9370		0.9410	
	P	0.8526	1.0000	0.8808	1.0000
		0.4711		0.8377	
Type II	Na	0.9399	0.9858	0.9611	0.9999
		0.9705		0.8398	
	Mg	0.9797	0.9992	0.9290	0.9998
		0.7591		0.9772	
	S	0.9753	0.9998	0.8352	0.9994
		0.9146		0.9042	
Type III	Ca	0.8005	0.9961	0.9641	0.9987
		0.9347		0.8776	
	Al	0.9875	0.9902	0.9323	0.9987
		0.9215		0.8650	
	Fe	0.9486	0.9663	0.9802	0.9978
		0.7520		0.8032	

R_1^2 is from first-order kinetic. R_2^2 is from second-order kinetic

of Na is greatly affected by the interaction between the leachate and CS. It is likely that the organic acids in the leachate favor the leaching of Na-containing compounds. The leaching of S follows the diffusion kinetics of the shrinking core model with a good regression coefficient R_1^2 of S higher than 0.91 at 20 ºC (Table 3). This leaching behavior is different from that of Na and Mg mainly due to the higher solubility of sulfates and other S-containing species that cannot react easily with the leachate. It can be seen (Fig. 3e and Table 3) that the R_2^2 of type II elements such as Na, Mg, and S using a second-order leaching model is always above 0.98 at 20 °C. Thus a reasonably good fit is obtained for type II elements.

It can be seen in Fig. 3c that the leaching of Ca among type III elements is controlled by the chemical reactions of the shrinking core model with the regression coefficient R_1^2 of Ca above 0.80 (Table 3). In contrast, Al and Fe's leaching kinetics fit the homogenous model with the regression coefficient R_1^2 of Al and Fe higher than 0.92 and 0.75, respectively. This observation indicates that the fit effect of Al among type III elements is the best. The leaching of Ca starts with the leaching of the water-soluble Ca salts on the surface of the CS particles, and then the leachate enters the inside of the CS particles and chemically reacts with CS. The latter process improves the leaching of Ca. Compared with the other two elements, Ca has a faster leaching rate in the first step. As can be seen from Fig. 3c, the leaching time of Al and Fe in the first step is 80 min, which may be related to the low solubility of compounds containing these two elements. In addition, the leaching of Al and Fe appears to be influenced by the composition and properties of the leachate. Furthermore, it can be seen (Fig. 3f and Table 3) that R_2^2 of the fitted data of type III elements (Ca, Al, and Fe) is always above 0.96 using a second-order leaching kinetic model. Compared with the first-order kinetics, this kinetic model exhibits greater regression coefficients.

The leaching kinetics of ash-forming elements at 50 ºC are shown in Fig. 4. The leaching of type I elements such as K, Cl, and P is controlled by the diffusion process of shrinking core model as shown in Fig. 4a at 50 ºC, where the R_1^2 of K, Cl, and P are always above 0.83 (Table 3). The reason for that is the high solubility of K, Cl, and P in CS in water. However, the leaching times of K and P in the first step are different. The duration of the first rapid leaching of K is shortened with increasing temperature due to the leaching of organic acid, which accelerates the leaching of K. Compared with 20 ºC, the leaching time of P in the first step is prolonged at 50 ºC. The reason for that is probably the competitive leaching among sulfate, carbonate, and phosphate anions. It can be seen (Fig. 4c and Table 3) that R_2^2 of the fitted data of type I elements (K, Cl, and P) using a second-order leaching model at 50 °C is the same as that at 20 °C. Their R_2^2 value is always 1.00 and greater than those of R_1^2 with the first-order kinetic model.

The leaching kinetics of ash-forming elements from type II and type III at 50 ºC were also investigated (Fig. 4b). The chemical reactions such as ion exchange and salt dissolution between the leachate and CS commonly enhance with increasing washing temperature. The leaching behavior of Na and Mg fit to chemical reactions controlled by shrinking core model with values of the regression coefficient R_1^2 higher than 0.83 and 0.92 at 50 ºC, respectively (Fig. 4b and Table 3). It is worth noting that Na's rapid leaching stage is shortened to 20 min at 50 ºC. Compared with the leaching at 20 ºC, the leaching kinetics of S at 50 ºC can still be explained by the shrinking core model with values of the regression coefficient R_1^2 higher than 0.83. Although the rate-determining step of S leaching is changed from diffusion control to chemical reaction control at 50 ºC, this observation does not mean that the diffusion process has stopped. Concurrently, the values of fitted kinetic parameters R_2^2 (Table 3 and Fig. 4d) demonstrate that R_2^2 of the type II elements (Na, Mg, and S) by the second-order leaching model is always above 0.99. These data show a better linear relationship than the shrinking core model.

Figure 4b clearly shows that the leaching behavior of type III elements (Ca, Al, and Fe) are controlled by chemical reactions at 50 ºC. Compared with 20 ºC, the leaching kinetic model of Ca is not changed, while the leaching kinetics of Al and Fe are changed from homogeneous model

to shrinking core model at 50 ℃. The change of the rate-determining steps of Al and Fe may be due to the enhanced interactions between some compounds in the leachate (such as organic acids and inorganic species) and CS with increasing temperature. These interactions show a positive effect on the leaching of Al and Fe. Analysis of the first-order and second-order leaching kinetic data (Fig. 4b and d) are carried out using Eqs.(7) and (11), respectively. The regression coefficient R_2^2 (above 0.99) of type III elements fitted by the second-order leaching kinetic model is higher than R_1^2 (above 0.80) of the shrinking core model. So, the second-order kinetic model is better suitable to describe the leaching kinetics of type III elements from CS.

The different concentrations of elements and their modes of occurrence in biomass are the main reasons for the leaching of ash-forming elements during the diffusion process. The analysis of the first-order leaching kinetics reveals that the diffusion process is the main factor affecting the leaching of type I elements (K Cl, and P) with high solubility. The leaching behavior of type II and type III ash-forming elements is mainly related to leachate and CS interactions. The different removal efficiency of ash-forming elements lead to leads to the leachate's charge imbalance during water washing. In this case, inorganic and organic substances on the CS surface or in the pores of the CS particles are susceptible to the electric field generated by the surrounding ions, also called the diffusion potential [40]. This will affect the leaching of certain inorganic and organic substances, thereby increasing the leaching of some ash-forming elements. With the prolongation of the washing time, the ash-forming elements' removal efficiency changes slightly and the dynamic leaching equilibrium is reached. In addition, these results presented generally low regression coefficients. The linearization is often better at the beginning of the process than at a later stage for the first-order kinetics. Compared with the first-order leaching model, the second-order leaching kinetics always presents greater regression coefficients at 20 °C and 50 °C (always above 0.96). This observation shows that the fitting effect of the second-order kinetics is better than that of the first-order kinetics of ash-forming elements from CS.

The commonly used two leaching models, namely the first-order kinetic model, including a homogeneous model and a shrinking nucleus model, or second-order kinetic model, were adopted to study the ash-forming elements' leaching. Correspondingly, the leaching rate constant, including the rate constant K_a of the homogeneous model, K_c of the reaction-control process, K_p of the diffusion-control process and K of the second-order kinetics, are compared, as shown in Table 4. The rate constant is an important physical quantity in chemical kinetics. Its value directly reflects the speed of the rate and it is not affected by the concentration of reactant, which reflects the rate characteristics of the reaction system. As illustrated in Table 4, it can be seen that the second-order kinetic rate constant is the biggest among four kinds of rate constants, which indicates that the reaction rate for the second-order reaction is faster than the first-order reaction during water leaching of CS.

Table 4 Comparison of the rate constants (K_a, K_c, K_p and K) of the first-order and second-order kinetic

Temperature		20 °C				50 °C		
Rate constant		K_a	K_c	K_p	K	K_c	K_p	K
Type I	K	-	-	-0.0012 -5.8067×10^{-5}	0.0247	-	-0.0017 -7.3977×10^{-5}	0.0382
	Cl	-	-	-0.0015 -7.2274×10^{-5}	1.3700	-	-0.0020 -7.1796×10^{-5}	0.6744
	P	-	-	-0.0049 -0.0001	0.6067	-	-0.0058 -1.3452×10^{-5}	0.1756
Type II	Na	-	0.0044 0.0004	-	0.0324	0.0053 0.0002	-	0.1708
	Mg	-	0.0047 0.0002	-	0.0202	0.0027 0.0001	-	0.0482
	S	-	-	-0.0067 -0.0002	0.0683	0.0017 0.0003	-	0.0438
Type III	Ca	-	0.0045 0.0004	-	0.0077	0.0054 0.0002	-	0.0121
	Al	0.0068 0.0006	-	-	0.1035	0.0035 0.0004	-	0.1991
	Fe	0.0042 0.0008	-	-	0.0920	0.0051 0.0004	-	0.1182

3.4 The effect of water washing on the ash-related problems during biomass gasification

The interactions between S, Cl and alkaline and alkaline-earth metals (AAEMs) in biomass are the critical factor affecting ash formation, transfer, and deposition during the gasification process. The risk of acid gas release, slagging and corrosion tendency during the practical thermal conversion can be predicted with the indices comprising S, Cl, and AAEMs. The commonly used parameters (in mole ratio) include S/Cl, (K + Na)/(2S + Cl), and Ca/(S + 0.5Cl) [41–43]. These indices were calculated based on the remaining ash-forming elements of the LCS. It can be seen from Fig. 5 that the three indices are almost not influenced by the washing temperature when the experimental error is considered.

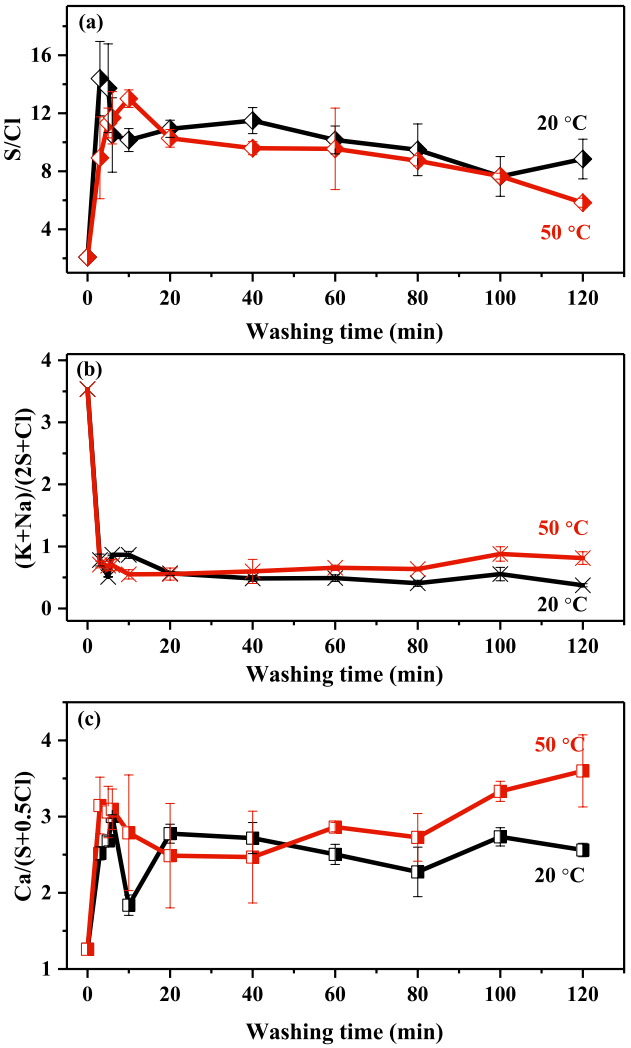

Fig. 5 Molar ratio of ash-forming elements from leached corn straw (a) S/Cl, (b) (K + Na)/(2S + Cl), (c) Ca/(S + 0.5Cl)

One of the measures to reduce chlorine-induced corrosion of the heat exchanger surface of the gasifier is to convert the alkali chlorides into less corrosive alkali sulphates by increasing the mole ratio of S/Cl. The S/Cl value above 4.0 is proposed to lower the corrosion risk [41]. It can be seen from Fig. 5a that the S/Cl of raw CS is 2 (< 4). It means that if the corn straw is used directly in the thermal conversion process, it could easily cause corrosion of the heat exchanger. The water washing technology can not only reduce the content of S and Cl but can also significantly increase the S/Cl ratio in LCS, which is far higher than 4.0 after water washing. It can also be predicted that the release of HCl, SO_2, SO_3, and other acid gases will be reduced during the LCS thermal conversion process, thereby alleviating the air pollution problem.

The initial gas-phase alkali concentration is related to the S and Cl results in grave slagging in both circulating fluidized bed and grate furnaces. Visser [42] proposed an agglomeration index based on the assumption that all of S and Cl present in the fuel reacts with the fuel alkali species. This author states that the agglomeration potential induced by alkali is high when (Na + K)/(2S + Cl) is > 1. It can be seen from Fig. 5b that the (K + Na)/(2S + Cl) is above 3 in the raw CS and is less than 1 after water washing. Hence, the water washing of corn straw can reduce the occurrence of alkali-induced agglomeration. It is worth noting that the washing time and temperature are favorable for the leaching of Na and S, but they had a limited effect on the molar ratio of (K + Na)/(2S + Cl).

Inorganic species like HCl and SO_2 are strongly dependent on the occurrence of Ca in the system [43]. For instance, the chemical equivalent ratio of Ca/(S + 0.5Cl) should be 1 to maintain the complete neutralization reactions based on the theoretical assumption for the consumption of $Ca(OH)_2$ by HCl and SO_2. As shown in Fig. 5c, the Ca/(S + 0.5Cl) in CS is close to 1 and then increases above 2 by water washing, which facilitates the release of Cl and S during the gasification process to transform the more corrosive HCl (g) and SO_2 (g) to the less corrosive $CaCl_2$ and $CaSO_4$ [44]. Figure 5c reveals that the Ca/(S + 0.5Cl) increases slightly with increasing temperature after 60 min at 50 ºC. It indicates that the higher washing temperature with a longer washing time is beneficial for inhibiting the production of acid gases during CS gasification.

The water washing can be effectively replicated for larger industrial applications with high pretreatment efficiency because it seems to be a prospective pretreatment process to remove a large part of troublesome elements from biomass fuels, thereby reducing the risk of ash deposition and improving gasification characteristics of biomass fuels [6, 45]. As per the experimental results, longer washing durations usually show a higher removal efficiency of ash-forming elements, but for industrial applications, a short time

(< 15–20 min) is more favourable [46]. The increase of washing temperature improves the removal efficiency of the ash-forming elements excluding Mg and P. To improve the removal efficiency of these elements, the washing temperature can be further increased for short washing durations. However, hot water requires even more energy to increase the temperature, which may lead to extra costs, so we need to choose a suitable temperature for washing pretreatment [47]. Biomass can be washed at the field or at the plant site. If washing is applied at the plant site, thus a pool must be constructed to collect the leachate for the recovery or reuse of wastewater produced by washing. If washing is applied at the field, water can be obtained from a river or lake nearby. The leachate from the pretreatment process, contains K, S, Cl and organic compounds that can be used to irrigate the field [6, 45, 46]. Another issue with the washed biomass is its high content of moisture, which limits its direct use in boilers and causes some handling and thermal conversion problems. Before entering the boiler, the washed biomass can be blended with woods, air-dried in the field or dried using hot stack gas to reduce the energy output [6, 45–47].

4 Conclusions

The leaching mechanisms of nine ash-forming elements (K, Na, Ca, Mg, Al, Fe, S, Cl, and P) in corn straw under different water washing conditions were elucidated in this study. The following conclusions can be drawn:

(1) The nine ash-forming elements studied can be categorized into three types. The type I elements include K, Cl, and P and they have a removal efficiency greater than 90% within 10 min. The type II elements are Na, Mg, and S with a removal efficiency greater than 70% and reach the leaching equilibrium within 120 min. The removal efficiency of the type III elements such as Ca, Fe, and Al is less than 63% within 120 min.
(2) The washing temperature and washing time have a limited effect on the leaching of K and Cl; however, the removal efficiency of the other ash-forming elements increases significantly with the washing time. The increase of washing temperature improves the removal efficiency of ash-forming elements excluding Mg and P. At high washing temperature (50 °C), the removal efficiency of Mg shows a decline tendency after 20 min, while P reveals a decline tendency for 10 min washing time.
(3) The leaching of ash-forming elements might be controlled by the first-order kinetic model, namely, homogeneous model and shrinking core model. Still, the second-order reaction model presents high regression coefficients, which is better suitable to fit the leaching kinetics of ash-forming elements from CS than the first-order kinetic leaching model. The reaction rate for the second-order reaction is faster than the first-order reaction during the water leaching of CS.
(4) The washing biomass technology can reduce the slagging tendency in the gasifier and the emission of acid gases.

Author contribution Data curation, formal analysis and writing-review & editing: Yuefeng Wang; Resources and validation: Shugang Guo; Data curation: Fang Cao; Validation: Chong He; Validation: Yuexing Wei; Writing-original draft, conceptualization and supervision: Yuhong Qin; Methodology: Yanyun He; Resources: Xing Du; Writing-review & editing: Stanislav V. Vassilev; Writing-review & editing: Christina G. Vassileva.

Funding The authors would like to thank the financial support from the National Natural Science Foundation of China (Grant No.: 21975172, 21776192) and the Natural Science Foundation of Shanxi Province (Grant No.: 20181D121282).

Declarations

Conflict of interest The authors declare no competing interests.

References

1. Knutsson P, Maric J, Knutsson J, Larsson A, Breitholtz C, Seemann M (2019) Potassium speciation and distribution for the K_2CO_3 additive-induced activation/deactivation of olivine during gasification of woody biomass. Appl Energy 248:538–544. https://doi.org/10.1016/j.apenergy.2019.04.150
2. Parvez M, Khan O (2020) Parametric simulation of biomass integrated gasification combined cycle (BIGCC) power plant using three different biomass materials. Biomass Convers Bior 10(4):803–812. https://doi.org/10.1007/s13399-019-00499-x
3. He Q, Guo Q, Ding L, Wei J, Yu G (2019) CO_2 gasification of char from raw and torrefy-ed biomass: reactivity, kinetics and mechanism analysis. Bioresour Technol 293:122087. https://doi.org/10.1016/j.biortech.2019.122087
4. Ge H, Zhang H, Guo W, Song T, Shen L (2019) System simulation and experimental verifi-cation: biomass-based integrated gasification combined cycle (BIGCC) coupling with chemic-al looping gasification (CLG) for power generation. Fuel 241:118–128. https://doi.org/10.1016/j.fuel.2018.11.091
5. Liaw SB, Wu H (2013) Leaching characteristics of organic and inorganic matter from biomass by water: differences between batch and semi-continuous operations. Ind Eng Chem Res 52(11):4280–4289. https://doi.org/10.1021/ie3031168
6. Deng L, Zhang T, Che D (2013) Effect of water washing on fuel properties, pyrolysis and combustion characteristics, and ash fusibility of biomass. Fuel Process Technol 106:712–720. https://doi.org/10.1016/j.fuproc.2012.10.006
7. Qin Y, He Y, Ren W, Gao M, Wiltowski T (2020) Catalytic effect of alkali metal in biom-ass ash on the gasification of coal char in

CO_2. J Therm Anal Calorim 139(5):3079–3089. https://doi.org/10.1007/s10973-019-08719-2
8. Vassilev SV, Baxter D, Andersen LK, Vassileva CG (2013) An overview of the composition and application of biomass ash. Part 1. Phase-mineral and chemical composition and classification. Fuel 105:40–76. https://doi.org/10.1016/j.fuel.2012.09.041
9. Vassilev SV, Vassileva CG (2019) Water-soluble fractions of biomass and biomass ash and their significance for biofuel application. Energ Fuel 33(4):2763–2777. https://doi.org/10.1021/acs.energyfuels.9b00081
10. Li H, Kong L, Bai J, Bai Z, Guo Z, Li W (2020) Modification of ash flow properties of coal rich in calcium and iron by coal gangue addition. Chinese J Chem Eng 28(11):2723–2732. https://doi.org/10.1016/j.cjche.2020.08.033
11. Yu C, Zheng Y, Cheng Y, Jenkins BM, Zhang R, Vandergheynst JS (2010) Solid-liquid extraction of alkali metals and organic compounds by leaching of food industry residues. Bioresource Technol 101(12):4331–4336. https://doi.org/10.1016/j.biortech.2010.01.074
12. Zeng T, Mlonka-Medrala A, Lenz V, Nelles M (2021) Evaluation of bottom ash slagging risk during combustion of herbaceous and woody biomass fuels in a small-scale boiler by principal component analysis. Biomass Convers Bior 11(4):1211–1229. https://doi.org/10.1007/s13399-019-00494-2
13. Yin J, Wu Z (2009) Corrosion behavior of TP316L of superheater in biomass boiler with simulated atmosphere and deposit. Chinese J Chem Eng 17(5):849–853. https://doi.org/10.1016/S1004-9541(08)60286-4
14. Jiao W, Wang Z, Jiao W, Li L, Zuo Z, Li G, Hao Z, Song S, Huang J, Fang Y (2020) Influencing factors and reaction mechanism for catalytic CO_2 gasification of sawdust char using K-modified transition metal composite catalysts: experimental and DFT studies. Energy Convers Manage 208:112522. https://doi.org/10.1016/j.enconman.2020.112522
15. Hu H, Westover TL, Cherry R, Aston JE, Lacey JA, Thompson DN (2017) Process simulation and cost analysis for removing inorganics from wood chips using combined mechanical and chemical preprocessing. BioEnerg Res 10(1):237–247. https://doi.org/10.1007/s12155-016-9794-3
16. Wu H, Yip K, Kong Z, Li C, Liu D, Yu Y, Gao X (2011) Removal and recycling of inherent inorganic nutrient species in mallee biomass and derived biochars by water leaching. Ind Eng Chem Res 50(21):12143–12151. https://doi.org/10.1021/ie200679n
17. Yu C, Thy P, Wang L, Anderson SN, VanderGheynst JS, Upadhyaya SK, Jenkins BM (2014) Influence of leaching pretreatment on fuel properties of biomass. Fuel Process Technol 128:43–53. https://doi.org/10.1016/j.fuproc.2014.06.030
18. Liu Q, Chmely SC, Abdoulmoumine N (2017) Biomass treatment strategies for thermochemical conversion. Energ Fuel 31(4):3525–3536. https://doi.org/10.1021/acs.energyfuels.7b00258
19. Yılmaz H (2015) Characterization and comparison of leaching behaviors of fly ash samples from three different power plants in Turkey. Fuel Process Technol 137:240–249. https://doi.org/10.1016/j.fuproc.2015.04.011
20. Cen K, Cao X, Chen D, Zhou J, Chen F, Li M (2020) Leaching of alkali and alkaline earth metallic species (AAEMs) with phenolic substances in bio-oil and its effect on pyrolysis characteristics of moso bamboo. Fuel Process Technol 200:106332. https://doi.org/10.1016/j.fuproc.2019.106332
21. Bakker RR, Jenkins BM (2003) Feasibility of collecting naturally leached rice straw for thermal conversion. Biomass Bioenerg 25(6):597–614. https://doi.org/10.1016/S0961-9534(03)00053-9
22. Saddawi A, Jones JM, Williams A, Le Coeur C (2012) Commodity fuels from biomass through pretreatment and torrefaction: effects of mineral content on torrefied fuel characteristics and quality. Energ Fuel 26(11):6466–6474. https://doi.org/10.1021/ef2016649
23. Gudka B, Jones JM, Lea-Langton AR, Williams A, Saddawi A (2016) A review of the mitigation of deposition and emission problems during biomass combustion through washing pre-treatment. J Energy Inst 89(2):159–171. https://doi.org/10.1016/j.joei.2015.02.007
24. Zevenhoven M, Yrjas P, Skrifvars BJ, Hupa M (2012) Characterization of ash-forming matter in various solid fuels by selective leaching and its implications for fluidized-bed combustion. Energ Fuel 26(10):6366–6386. https://doi.org/10.1021/ef300621j
25. Werkelin J, Skrifvars BJ, Zevenhoven M, Holmbom B, Hupa M (2010) Chemical forms of ash-forming elements in woody biomass fuels. Fuel 89(2):481–493. https://doi.org/10.1016/j.fuel.2009.09.005
26. Deng L, Che D (2012) Chemical, electrochemical and spectral characterization of water leachates from biomass. Ind Eng Chem Res 51(48):15710–15719. https://doi.org/10.1021/ie301468b
27. Arvelakis S, Gehrmann H, Beckmann M, Koukios EG (2005) Preliminary results on the ash behavior of peach stones during fluidized bed gasification: evaluation of fractionation and leaching as pre-treatments. Biomass Bioenerg 28(3):331–338. https://doi.org/10.1016/j.biombioe.2004.08.016
28. Davidsson KO, Korsgren JG, Pettersson JBC, Jäglid U (2002) The effects of fuel washing techniques on alkali release from biomass. Fuel 81(2):137–142. https://doi.org/10.1016/S0016-2361(01)00132-6
29. Stanković V, Gorgievski M, Božić D (2016) Cross-flow leaching of alkali and alkaline-earth metals from sawdust and wheat straw-modelling of the process. Biomass Bioenerg 88:17–23. https://doi.org/10.1016/j.biombioe.2016.03.013
30. Madanayake BN, Gan S, Eastwick C, Ng HK (2016) Leaching as a pretreatment process to complement torrefaction in improving co-firing characteristics of Jatropha curcas seed cake. Waste Biomass Valori 7(3):559–569. https://doi.org/10.1007/s12649-015-9467-z
31. Ho YS, Harouna-Oumarou HA, Fauduet H, Porte C (2005) Kinetics and model building of leaching of water-soluble compounds of *Tilia* sapwood. Sep Purif Technol 45(3):169–173. https://doi.org/10.1016/j.seppur.2005.03.007
32. Schmidt G, Trouvé G, Leyssens G, Schönnenbeck C, Brillard A, Olya ME, Dewaele D, Cazier F (2020) Influence and modelling of wood washing on mineral and organic compositions of three woods (beech, fir and oak). J Energy Inst 93(1):198–209. https://doi.org/10.1016/j.joei.2019.03.008
33. Huang Y, Zhao Y, Hao Y, Wei G, Feng J, Li W, Yi Q, Mohamed U, Pourkashanian M, Nimmo W (2019) A feasibility analysis of distributed power plants from agricultural resid-ues resources gasification in rural China. Biomass Bioenerg 121:1–12. https://doi.org/10.1016/j.biombioe.2018.12.007
34. Wang X, Wu H, Dai K, Zhang D, Feng Z, Zhao Q, Wu X, Jin K, Cai D, Oenema O, Hoogmoed WB (2012) Tillage and crop residue effects on rainfed wheat and maize production in northern China. Field Crops Res 132:106–116. https://doi.org/10.1016/j.apenergy.2019.04.150
35. Irfan MF, Usman MR, Rashid A (2018) A detailed statistical study of heterogeneous, homogeneous and nucleation models for dissolution of waste concrete sample for mineral carbonation. Energ 158:580–591. https://doi.org/10.1016/j.energy.2018.06.020
36. Li L, Bian Y, Zhang X, Guan Y, Fan E, Wu F, Chen R (2018) Process for recycling mixed-cathode materials from spent lithium-ion batteries and kinetics of leaching. Waste Manage 71:362–371. https://doi.org/10.1016/j.wasman.2017.10.028
37. Martínez-Luévanos A, Rodríguez-Delgado MG, Uribe-Salas A, Carrillo-Pedroza FR, Osuna-Alarcón JG (2011) Leaching kinetics of iron from low grade kaolin by oxalic acid solutions. Appl Clay Sci 51(4):473–477. https://doi.org/10.1016/j.clay.2011.01.011

38. Bandara YW, Gamage P, Gunarathne DS (2020) Hot water washing of rice husk for ash removal: The effect of washing temperature, washing time and particle size. Renew Energ 153:646–652. https://doi.org/10.1016/j.renene.2020.02.038
39. Vassilev SV, Baxter D, Andersen LK, Vassileva CG, Morgan TJ (2012) An overview of th-e organic and inorganic phase composition of biomass. Fuel 94(1):1–33. https://doi.org/10.1016/j.fuel.2011.09.030
40. Tsai SC, Lee E (2019) Diffusiophoresis of a highly charged porous particle induced by diffusion potential. Langmuir 35(8):3143–3155. https://doi.org/10.1021/acs.langmuir.8b04146
41. Galanopoulos C, Yan J, Li H, Liu L (2018) Impacts of acidic gas components on combust-ion of contaminated biomass fuels. Biomass Bioenerg 111:263–277. https://doi.org/10.1016/j.biombioe.2017.04.003
42. Visser HJM (2004) The influence of fuel composition on agglomeration behaviour in fluidised bed combustin. ECN-C-04–054 44.
43. Porbatzki D, Stemmler M, Müller M (2011) Release of inorganic trace elements during ga-sification of wood, straw, and miscanthus. Biomass Bioenerg 35:S79–S86. https://doi.org/10.1016/j.biombioe.2011.04.001
44. Wu D, Wang Y, Wang Y, Li S, Wei X (2016) Release of alkali metals during co-firing biomass and coal. Renew Energy 96:91–97. https://doi.org/10.1016/j.renene.2016.04.047
45. Guo Q, Cheng Z, Chen G, Yan B, Hou L, Ronsse F (2020) Optimal strategy for clean and efficient biomass combustion based on ash deposition tendency and kinetic analysis. J Clean Prod 271:122529. https://doi.org/10.1016/j.jclepro.2020.122529
46. Singhal A, Konttinen J, Joronen T (2021) Effect of different washing parameters on the fu-el properties and elemental composition of wheat straw in water-washing pre-treatment Part 2 Effect of washing temperature and solid-to-liquid ratio. Fuel 292:120209. https://doi.org/10.1016/j.fuel.2021.120209
47. Singhal A, Goossens M, Konttinen J, Joronen T (2021) Effect of basic washing parameters on the chemical composition of empty fruit bunches during washing pretreatment: A detailed experimental, pilot, and kinetic study. Bioresource Technol 340:125734. https://doi.org/10.1016/j.biortech.2021.125734